مجلة جمعية الليزر العراقية
Iraqi Laser Society Journal
I.L.S.J.
Issue-2 3rd Year 2026

Simulation Design of Photonic Crystal Fiber (PCF) Laser for Optical Communication Application

Ban M. Al Bayati, Aseel I. Mahmod, Esraa K. AL-Gazzi, and Lubna G. Abdulatif

Ministry of Higher Education and Scientific Research/ Scientific Research Commission, Baghdad, Iraq

Email: ban.m.saed@src.ed.iq; dr.banalbayati22@gmail.com

Abstract

This work presents the simulation design of a hexagonal Photonic Crystal Fiber (PCF) laser tailored for optical communication applications. Utilizing the Finite Element Method through COMSOL Multiphysics (6.1) simulation software, to study the optical characteristics of the proposed PCF structure, including effective refractive index (n_{eff}), confinement loss (L_c), effective mode area (A_{eff}), nonlinear coefficient (γ), and dispersion. The influence of infiltrating the PCF air holes with varying refractive indices (1.0, 1.33, 1.354, 1.37, and 1.39) on laser performance was systematically analyzed. The results demonstrate a Gaussian-shaped laser output with stable intensity profiles over a wavelength range of 1200 nm to 2000 nm. This wide operational bandwidth and the tunable design make the proposed PCF laser a promising candidate for advanced optical communication systems.

Keywords: photonic crystal fiber laser, optical communication, simulation model PCFL, fiber laser design

مجلة جمعية الليزر العراقية
Iraqi Laser Society Journal
I.L.S.J.

Issue-2 3rd Year 2026

نمذجة تصميم ليزر الليف البلوري الكرستالي وتطبيقه في الاتصالات البصرية

بان مظفر البياتي واسيل ابراهيم محمود و اسراء كامل الغازي و لبنى غازي عبد اللطيف

وزارة التعليم العالي والبحث العلمي /هيئة البحث العلمي،بغداد،العراق

Email: ban.m.saed@src.ed.iq; dr.banalbayati22@gmail.com

الخلاصة

يقدم هذا البحث تصميم محاكاة ليزر يعتمد على الألياف البصرية البلورية الضوئية السداسية (PCF) مخصصًا لتطبيقات الاتصالات الضوئية. تم الاعتماد على طريقة العناصر المحددة باستخدام برنامج COMSOL Multiphysics 6.1 لدراسة الخصائص البصرية للهيكل المقترح، وتتضمن معامل الانكسار الفعّال(neff) ، فقدان الحجز(Lc) ، مساحة الوضع الفعّالة(Aeff) ، المعامل غير الخطي(γ) ، والتشتت. تم تحليل تأثير إدخال معاملات انكسار مختلفة (1.0، 1.33، 1.354، 1.37، و1.39) في الفجوات الهوائية داخل الألياف البصرية على أداء الليزر بشكل منهجي. أظهرت النتائج مخرجات ليزر ذات شكل غاوسي واستقرار في شدة الإشعاع على معدل طول موجي يمتد من 1200 نانومتر إلى 2000 نانومتر. هذا النطاق العريض ومرونة التصميم يجعل ليزر PCF المقترح مرشحاً واعداً لانظمة الاتصالات البصرية المتقدمة.

الكلمات المفتاحية: ليزر الليف البصري البلوري، الاتصالات البصرية، تصميم نمذجي لليزر الليف البصري البلوري، تصيم ليزر الالياف

Introduction:

In the last ten years, rare-earth-doped fiber lasers and amplifiers have become a leading architecture for high-power solid-state laser systems. Due to major technological progress, these systems can now achieve kilowatt-level continuous-wave outputs while maintaining exceptional beam precision. [1][2][3]. Such performance milestones are primarily attributable to the unique inherent properties of active fibers, which facilitate efficient thermal management and robust spatial mode control. The performance advantages of waveguide-structured lasers are primarily derived from efficient pump confinement and guided radiation. In these systems, the laser output mode quality remains largely independent of power, Its core nature is determined by the specific refractive-index distribution within the doped fiber core. Furthermore, fiber lasers are essentially immune to thermo-optic distortions due to their high surface-to-active-volume ratio, which ensures efficient heat dissipation. The exceptional single-pass gain found in rare-earth-doped fibers is a direct result of efficient pump radiation confinement. This "robust guiding" ensures that the pump light remains highly concentrated over a long distance, maximizing the interaction between the light and the fiber material. However, this tight spatial confinement—typically within a mode-field diameter of ~10 µm for conventional single-mode fibers—combined with extended interaction lengths (ranging from 1 m to 100 m) significantly lowers the threshold for parasitic nonlinear effects, such as stimulated Raman scattering (SRS) and self-phase modulation (SPM) [4]. The main limitation for increasing the power of fiber lasers and amplifiers is the onset of nonlinear effects. Because the threshold for these effects is determined by the ratio of the mode-field area (MFA) to the fiber length, performance can be greatly improved by using shorter fibers with larger cores. In this study, we present a unique large-mode-area (LMA) photonic crystal fiber (PCF) that bridges the gap between traditional fiber lasers and rod-type laser dimensions. Using a remarkably short 48 cm fiber, we generated 120 W of single-mode output power at a 74% slope efficiency. This results in an extraction rate of 250 W/m, which, as far as we are aware, represents a new record for fiber laser systems. [5].

Photonic crystal fibers (PCFs) and fiber lasers are among the fastest-growing fields in optics and photonics. Recent advancements in PCFs have revolutionized light generation, manipulation, and transmission, offering new opportunities for fiber laser design. These developments are influencing the performance, functionality, and application range of fiber lasers. This review explores how PCFs are shaping the evolution of fiber laser technologies and their potential future impact on various industries [6]. The integration of large-mode-area designs with air-clad microstructured architectures represents a significant milestone in fiber laser technology. By utilizing sub-wavelength silica bridges to confine pump radiation, these fibers achieve a high pump-core numerical aperture, facilitating the transition to kilowatt-level continuous-wave operation. However, as power levels continue to rise, the interplay between the mode-field area and the fiber length remains critical, as nonlinearities—rather than thermal damage—emerge as the primary bottleneck for further scaling. As noted by Chen et al.,[7] high-power fiber lasers have advanced rapidly following the development of rare-earth-doped double-clad fibers. However, further power scaling is fundamentally constrained by nonlinear effects, thermal management challenges, and material damage thresholds. Photonic crystal fibers (PCFs) offer a viable solution to these limitations by providing a significantly increased large mode area (LMA) and a low-effective-index core. This study presents a simplified and versatile fabrication method for ytterbium-doped double-clad (YDDC) PCFs, designed to mitigate these performance bottlenecks. Numerical simulations and experimental characterizations confirm the robust performance of the fabricated fibers, which achieved a laser slope efficiency exceeding 86.8%. These results underscore the significant potential of the proposed fabrication technique for high-power fiber laser systems. Specifically, the high efficiency and experimental stability suggest that this simplified approach provides a scalable pathway for developing next-generation ytterbium-doped double-clad (YDDC) PCFs [7]. In 2023, Rahman et al. developed a hexagonal photonic crystal fiber (H-PCF) featuring a rotational hexa-elliptical core, modeled using COMSOL Multiphysics. Designed for terahertz (THz) telecommunications, the cladding architecture consists of five layers of circular air holes. The H-PCF was optimized to achieve an ultra-low Effective Material Loss (EML), enhanced core power fraction, a large effective area, and minimized confinement loss. Numerical results at the THz waveguide region demonstrated an ultra-low EML of 0.00689 cm-1, a core power fraction of

82%, and a confinement loss of 3.45× 10^{-14} cm^{-1} with an effective area of 3.65 × 10^{-4} m^2. Furthermore, the design maintains single-mode operation across the targeted THz spectrum, establishing the H-PCF as a highly viable candidate for high-speed optical fiber communications [8]. Maidi et al. (2021) investigated a hexagonal lattice PCF model where the core was infiltrated with benzene, ethanol, and water to evaluate its sensing performance. The proposed architecture features a cladding with three concentric rings of air holes, while the core incorporates three identical air holes to enhance light-matter interaction. To evaluate the fiber's optical characteristics, we employed a full-vector finite element method (FEM) analysis integrated with anisotropic perfectly matched layers (PMLs). The numerical results demonstrate that this design offers high relative sensitivity, a high-power fraction, and low chromatic dispersion. Furthermore, it exhibits low confinement loss and a high nonlinear coefficient across a broad spectral range of 0.6–1.8 µm. Specifically, at an operating wavelength of 1.3 µm, the relative sensitivities for benzene, ethanol, and water were 74.50%, 65.34%, and 62.60%, respectively, with corresponding nonlinear coefficients of 95.4, 73.8, and 69.4 $W^{-1}km^{-1}$. The study concludes that this simplified structure is both conducive to fabrication and highly effective for liquid-phase chemical detection [9].

Fiber Optical Technology

Light is guided and confined using optical fibers, which function as dielectric waveguides. [10]. The three primary elements of a fiber optic are the coating or buffer, the cladding, and the core. As shown in figure (1).

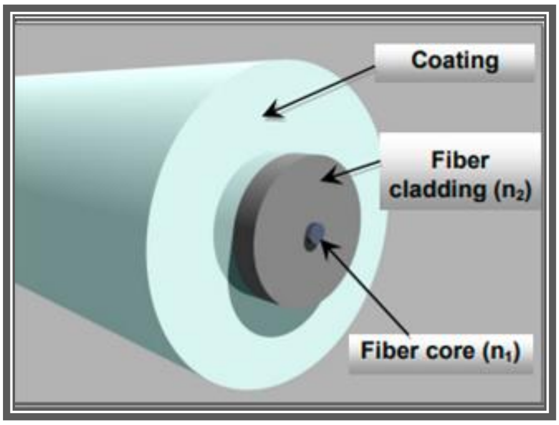

Figure (1) Basic structure of an optical fiber [4].

Typically composed of glass, the cylindrical center portion (the core) is made of a dielectric material. with a diameter ranging from 5 µm to 100 µm. Light mostly travels via the fiber's center. [4]. The dielectric cladding possesses a refractive index that is less than the refractive index of the core [11], and generally made of glass or plastic. The majority of fibers have cladding that is between 125 and 200 meters in diameter. An optical fiber is shielded from physical harm by a coating or buffer, which is a layer composed of an elastic plastic that resists abrasions [4].

An optical fiber guided light with wavelengths of infrared and visible light using a phenomenon called TIR where two different materials meet, and each has a unique refractive index. The refractive index of core is more than the claddings. This indicates that the interface, or border, between the cladding and the core functions as a perfect mirror. Light confined by that mirror and traveling along the core [11], The acceptance angle (θa) at the air-fiber tip interface can be calculated using Snell's Law, which must be applied to both the point where light enters the fiber (air-fiber tip) and the core-cladding boundary. given by equation (1) [12].

$$\theta a = \sin^{-1} (NA) \;\ldots\ldots\; (1)$$

$$NA = \sqrt{(n_1^2 - n_2^2)} \;\ldots\ldots\; (2)$$

The term NA, or Numerical Aperture, quantifies the light-gathering ability of the optical fiber. This value is determined by the refractive index of the core n1 and the refractive index of the cladding n2.

While conventional optical fibers work well in various applications, including telecommunications, their structure presents certain drawbacks or constraints. To ensure proper operation, these fibers are subject to rigorous design constraints. Specifically, they must maintain a core diameter small enough to support only single-mode propagation, satisfy specific modal cut-off wavelength criteria, and operate within a limited range of compatible materials (core and cladding glass must have identical thermal properties). PCF (Photonic Crystal Fiber) designs offer extraordinary flexibility. Several parameters can be easily adjusted, including the lattice pitch (spacing), the diameter and shape of the air holes, the refractive index of the glass, and the type of lattice arrangement used. These are single-mode fibers that operate across the entire optical spectrum without a cut-off wavelength, can be created thanks to design freedom [13]

- **Photonic Crystal Fibers (PCFs)**

PCFs (also called holey fiber, microstructure fiber, or micro structured fiber) is a new type of optical fiber having an internal periodic structure composed of air-filled capillaries arranged in a hexagonal lattice. Defects in the fiber's crystal structure allow light to travel along it. Removing one or more central capillaries results in a defect. Combining characteristics of photonic crystals and optical fibers, they have a number of special qualities that are not feasible with traditional fibers. [6]

The PCF design is powerful because of its great versatility in shape, function, and composition. Therefore, there is a high interest of the scientific community in employing all kind of (PCFs)[Thévenaz, 2011]

The (PCFs) could be designed depending on the cladding structure, the air hole), size (diameter (d), and the pitch, also known as the hole-to-hole spacing, is the separation between the centers of two adjacent air holes, as seen in the figure (2). Another often used characteristic is the relative hole size (d/), which is defined as the ratio of the air hole size to the pitch spacing. The air filling is another metric that is frequently used to characterize PCFs. The area of the air holes divided by the area of the silica in the cladding is known as the fraction (AFF). Compared to normal fibers with a circular core, it is more difficult to define the core diameter in PCFs. However, the core diameter of hexagonal PCFs with a single air hole defect is frequently expressed as (2-d), as seen in figures (3). [14]

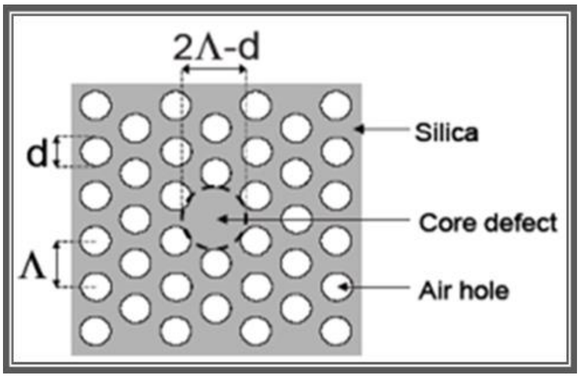

Figure (2): Cross section of photonic crystal fiber [14].

The Photonic Crystal Fibers can be classified into two main groups as shown in figure (3):

1- SC-PCFs, which are Photonic Crystal Fibers that have a non-hollow core.

2- HC-PCFs, which are Photonic Crystal Fibers distinguished by their empty core.

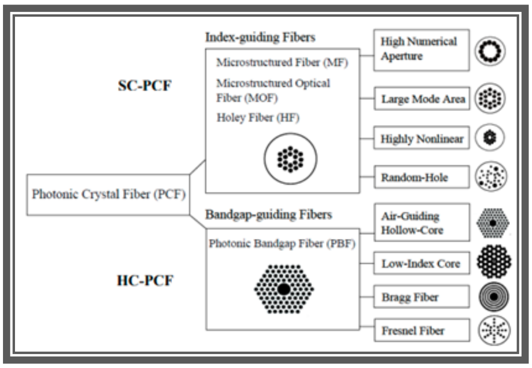

Figure (3) The classification of photonic crystal fiber [15]

The Propagation Properties through PCFs

- **Cladding effective index (n_{eff})**

Mirroring the mechanism of conventional fibers, this fiber operates on the principle of total internal reflection (TIR), as the core possesses a higher refractive index than the effective index of the surrounding cladding. Light in the core can use the propagation constants β, whereas light propagating in the cladding cannot and it is shown in equation (3) [16]

$\beta_{FSM} < \beta < K_{n_o}$…… (3)

Where (k=2π/λ), (n_o) is the index of silica (the core material), and (β_{FSM}) is the propagation constant of the Fundamental Space-filling Mode (FSM).

The greatest (β) permitted in the cladding is (β_{FSM}), since the FSM is the fundamental mode, the effective cladding index n_{eff} was calculated by analyzing the FSM is the fundamental mode The FSM is the lowest-order mode of the pure photonic crystal cladding and provides the lowest possible value for the propagation constant (β) if the core were removed. Since the cladding's [16]:

$n_{eff} = \beta_{FSM} / k$ ………….(4)

- **Effective Mode Area (A_{eff})**

The effective mode area A_{eff} is a critical metric, used to gauge non-linear effects in the fiber. A smaller effective mode area results in a higher power density, which is necessary for these non-linear effects to become noticeable [4]. Additionally, the effective area (A_{eff}) is linked to the mode field radius (or spot size, (w) by the relation $A_{eff} = 2\pi w^2$ Consequently, this parameter is a vital factor in determining various performance metrics, including confinement and bending losses (both micro and macro), as well as splicing efficiency and the fiber's numerical aperture. [17].

$$A_{eff} = \frac{\left(\iint_s |E|^2 \, dx\, dy\right)^2}{\iint_s |E|^4 \, dx\, dy} \ (\mu m^2) \ …. (5)$$

E which represents how the electrical field is distributed is determined by solving an eigenvalue equation rooted in the fundamental principles of Maxwell's equations. It's feasible to greatly increase the effective area by narrowing the air-holes for a fixed pitch (ʌ), or by widening the pitch for a fixed normalized air hole size (d/ʌ) value and then achieve radically different attributes of PCF [18].

- **Confinement Losses (Lc)**

Confinement loss is a type of light leakage in PCFs that indicates how well the core can hold the light. It occurs because the number of air-hole rings is finite, allowing the optical mode to escape (leak) from the core, passing through the bridges between the air holes and into the surrounding material as it travels. The following formula is used to determine confinement loss Lc in dB/km[19]:

$$L_C = \frac{2\pi\left(\frac{20}{\ln 10}\right) Im(n_{eff})}{\lambda} = 8.686\frac{2\pi}{\lambda} Im\ (n_{eff}) \ ……(6)$$

The imaginary part of the refractive index is Im (n_{eff}) and (λ) the wavelength. Confinement loss decreases exponentially as more layers of air holes are added to the cladding, with the total loss ultimately determined by the fiber's specific geometric arrangement [19].

- **Non-Linear coefficient (γ)**

The non-linearity coefficient γ is given by [4]

$$\Upsilon = \frac{n_2\,W}{c\,A_{eff}} = \frac{n_2\,2\pi}{\lambda A_{eff}} \quad \ldots\ldots\ldots\ldots (7)$$

Where: (n_2) the nonlinear-index coefficient in the nonlinear part of the refractive index. Understanding the non-linear phenomena (Aeff) within Photonic Crystal Fibers (PCFs) is essential. The large index contrast between the silica material and the air holes is what gives PCFs the ability to confine the light mode much more tightly over an extensive spectrum, resulting in a reduced effective mode area compared to conventional fibers. Furthermore, the air-holes cladding of the (PCFs) also allows for zero-dispersion engineering [20]

- **Transmission function T [21]**

The transmittance spectrum can be evaluated by using the following equation

$$T_{r\,(dB)} = 10 * \log_{10}\left(\frac{P_{out}}{P_{in}}\right) \ldots\ldots (8)$$

where T_r is the transmission of light, and Pin is the maximum power as a fraction of P_{out} [22].

- **Dispersion equation**

Dispersion D is the measure of the light guiding capabilities of the fiber, which is defined as [23][16]

$$D = -\frac{\lambda}{c}\frac{d^2}{d\lambda^2}\,\mathrm{Re}[n_{eff}] \ldots\ldots (9)$$

This formula involves λ which is the operating wavelength, c is the speed of light in a vacuum, and the real part of the effective refractive index $\mathrm{Re}[n_{eff}]$.

Simulation Results and Discussion

The finite element method (FEM) was implemented using COMSOL Multiphysics to solve Maxwell's equations and analyze light propagation within the optical fiber. Perfectly Matched Layers (PML) were employed as boundary conditions to ensure accurate absorption of outgoing waves and prevent spurious reflections, thereby maintaining confinement of the optical field within the fiber core. An extra-fine mesh was utilized to achieve high spatial resolution and enhance the precision of computed parameters, including the effective refractive index . The simple hexagonal lattice photonic crystal fiber with solid core surrounded with air holes diameters as shown in figure (4)

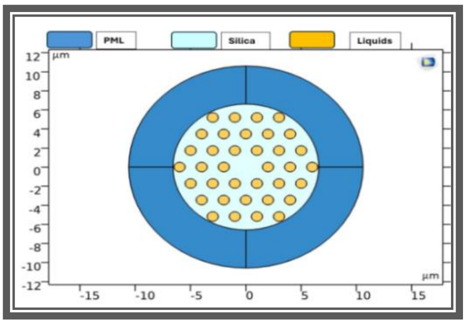

a

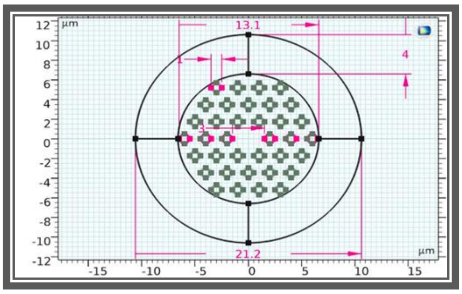

b

Figure (4) The design of photonic crystal fiber; a- represent the hexagonal shape of PCF material; b- hexagonal shape PCF geometry.

The design solid core photonic crystal fiber has a pitch (hole to hole spacing (Λ) about 3µm, air hole diameter (d) about 1 µm, the perfectly matched layer (PML thickness equal 4 µm), the diameter of hole area (D) equal 13.1 µm and the diameter of photonic crystal fiber equal 21.2 µm. To enhance the absorption of the reflected light the perfectly matched layer (PML) boundary condition is applied to this mode. The thickness of PML layer is 4 µm and the material is silica.

In our experiment used the refractive index 1, 1.33, 1.35, 1.37 and 1.39 as shown in figure (5) they show the fundamental mode propagating within the fiber core is

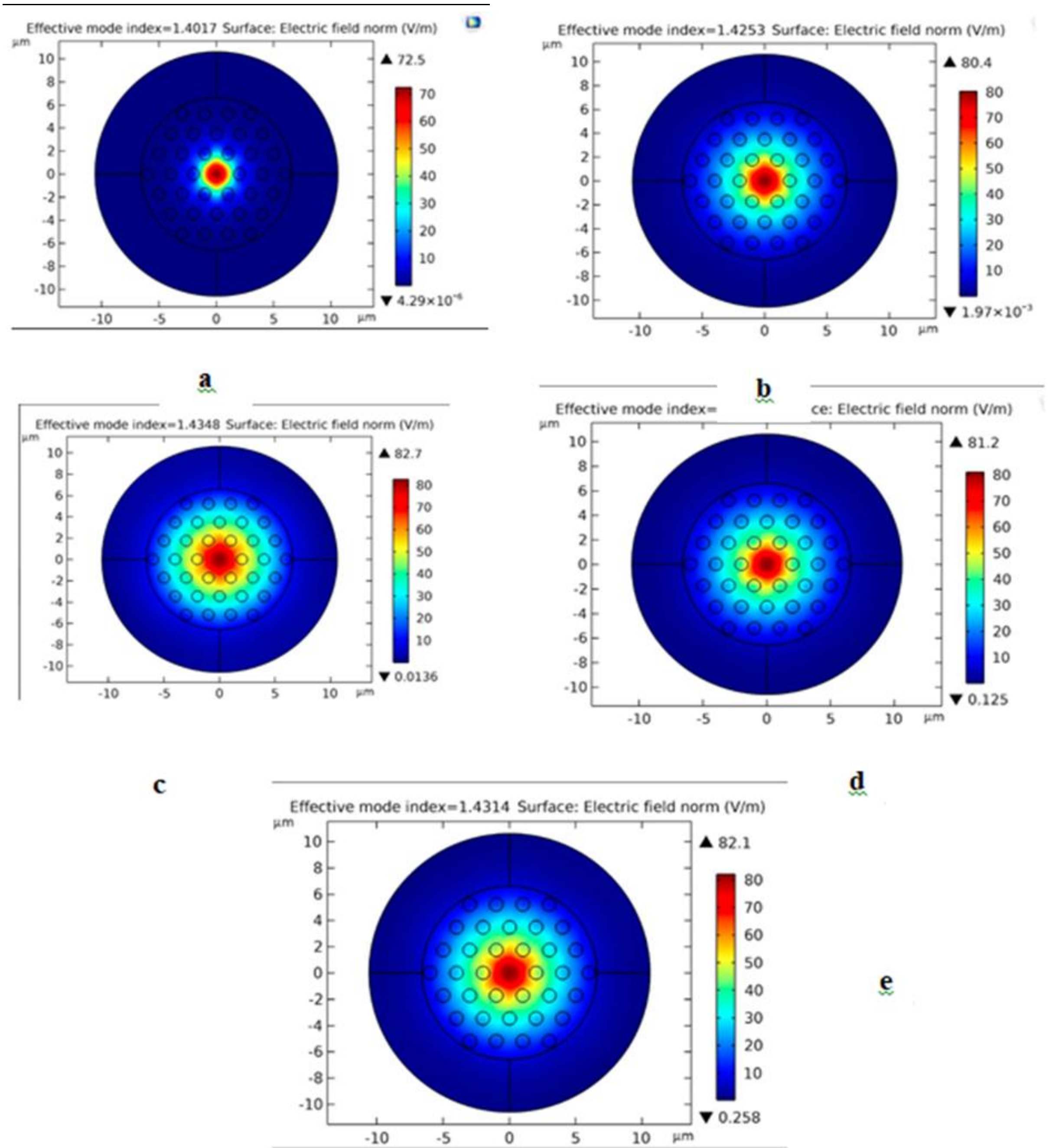

Figure (5) the electric field distribution with different refractive index

a-n=1; b- n= 1.33; c- n=1.35; d- n=1.37; e- n=1.39

represented by the core mode. In our project Refractive indices in the range of 1.33–1.39 were selected to emulate realistic variations encountered in photonic crystal fiber (PCF)–based optical communication systems. This interval corresponds to prevalent liquid and polymeric materials commonly employed for infiltration within PCF structures to enable tunable optical characteristics. Such controlled variation facilitates rigorous analysis of effective refractive index, modal confinement, and chromatic dispersion—parameters that critically influence the performance and sensitivity of advanced optical communication architectures. The effective refractive index (n_{eff}) is decreasing with increasing the wavelength for the different refractive index as shown in figure (6) the reasons of decreasing n_{eff} with increasing wavelength from the material dispersion of the core and cladding materials; Changes in waveguide dispersion due to mode spreading; and increased interaction with low-index regions in the cladding. This behavior is important for understanding dispersion engineering, mode confinement, and light propagation in photonic crystal fibers, especially in applications like super continuum generation and nonlinear optics.

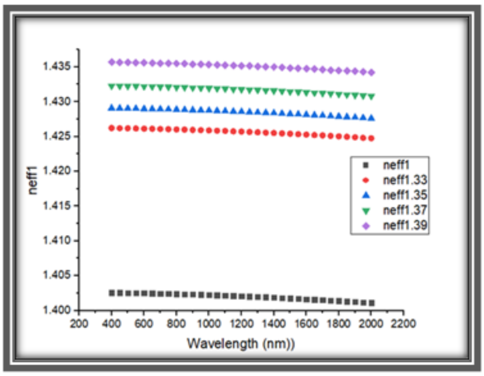

Figure (6) The relation between the effect refractive index (neff) and wavelength.

The area mode effective are calculated by equation (5) the effective mode area is increasing with increasing wavelength with different refractive index as shown in figure (7).

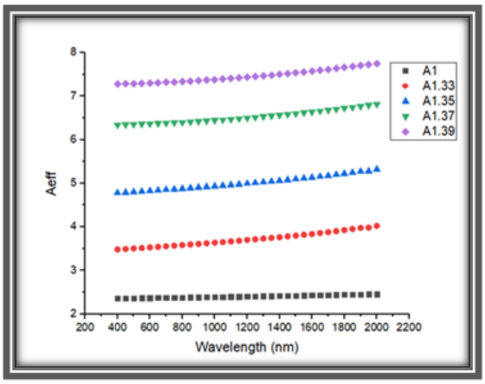

Figure (7) The relation between the area effective (A(eff)) and wavelength

The increase in the effective mode area with wavelength arises from the mode expansion due to weaker confinement at longer wavelengths. The wavelength dependence of material dispersion, waveguide dispersion, and refractive index contrast. Scaling properties inherent to the wavelength and waveguide structure. This behavior is crucial for designing Photonic crystal fiber for applications like super continuum generation, nonlinear optics, and high-power laser systems.

In figure (8) the Confinement loss increases with wavelength exponentially due to weaker confinement of the optical mode, mode expansion, and increased interaction with the cladding or air holes. Refractive index variation among the curves indicates that higher refractive index contrasts lead to different levels of confinement loss, influenced by the balance between core- cladding contrast and the wavelength dependent guiding mechanism.

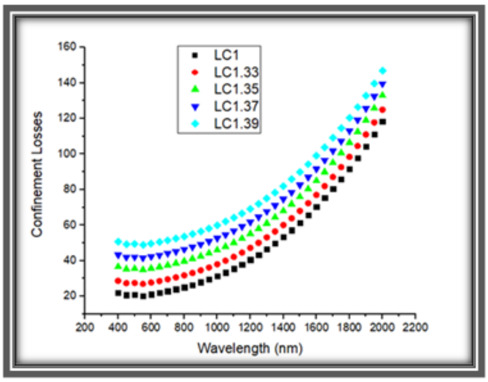

Figure (8) The relation between the confinement losses and wavelength

The nonlinear coefficient (γ) are calculated by equation (7) as it clear from the equation that the γ inversely proportional with A_{eff} and is it decrease with the increasing of wavelength as shown in figure (9)

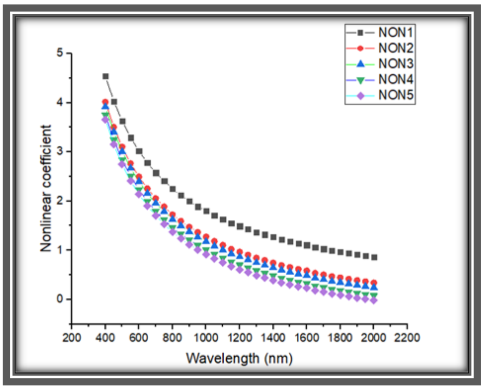

Figure (9) The relation between the nonlinear coefficient and wavelength

The total dispersion as it mentioned before is consist of two parts. The first part is the waveguide dispersion which has been calculated from the real part value of the effective refractive index as a function of wavelength as it clear from Equation (9) cladding index decreases. The dispersion characteristics for various PCF configurations were calculated and are illustrated in Figure (10). At shorter wavelengths, the mode remains tightly localized within the silica core; however, as the wavelength increases, the effective refractive index of the cladding begins to decline.

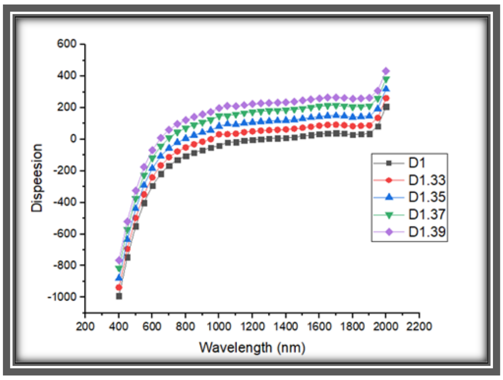

Figure (10) The relation between the dispersion and wavelength

The output powers of photonic crystal fiber laser are calculated by the equation (8). The output of asers have a Gaussian shape as shown in the figure (11).

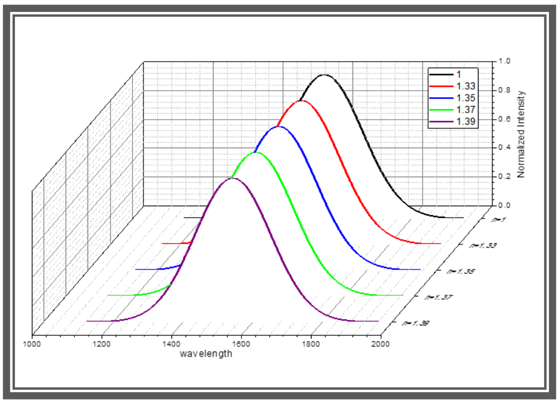

Figure (11) The relation between the normalized intensity and wavelength

The results of lasers intensity are matched for all value of refractive index. The band of laser of wavelength from (1200 to 2000) nm and the peak of intensity equal 0.99 at wavelength 1.540 nm this band of wavelength were made the laser output could be used in many applications specially in the optical communication. Chen et. Al., 2025 were presented a compact plasmonic polarization filter based on a gold-coated photonic crystal fiber, designed and analyzed using the finite element method. The filter operates at the 1.55 μm optical communication window and demonstrates excellent performance, including an extremely high extinction ratio, broad bandwidth, and very low insertion loss within a short fiber length. Owing to its simple structure and compatibility with existing fabrication techniques, the proposed all-fiber device shows strong potential for applications in optical communication, lasers, sensing, biomedicine, and nonlinear optics [24].

Conclusion

The simulated laser output demonstrates a well-defined Gaussian intensity profile, indicating high beam quality and efficient energy confinement within the photonic crystal fiber. The results confirm that the hexagonal PCF laser can be effectively optimized to operate over a broad near-infrared wavelength range from 1200 to 2000 nm, which is highly relevant for optical communication applications. Furthermore, the stable laser performance observed under varying refractive index conditions highlights the structural flexibility and adaptability of the proposed design to different material configurations and environmental variations. The comprehensive analysis of key optical parameters enables precise control of the laser characteristics, including emission bandwidth, intensity distribution, modal behavior, and nonlinear response. These features position the proposed hexagonal PCF laser as a promising platform for advanced fiber-based applications such as optical communications, sensing, and spectroscopy

References

[1] Y. Jeong, J. K. Sahu, D. Payne, and J. Nilsson, “Ytterbium-doped large-core fiber laser with 1 kW CW output power,” in Advanced Solid-State Photonics, G. J. Quarles, Ed., OSA Trends in Optics and Photonics Series, vol. 94, Postdeadline Paper PD1. Washington, DC, USA: Optical Society of America, 2004.

[2] C.-H. Liu, A. Galvanauskas, B. Ehlers, S. Heinemann, A. Carter, K. Tankala, and J. Farroni, “810-W single transverse-mode Yb-doped fiber laser,” in Advanced Solid-State Photonics, G. J. Quarles, Ed., OSA Trends in Optics and Photonics Series, vol. 94, Postdeadline Paper PD2. Washington, DC, USA: Optical Society of America, 2004.

[3] A. Liem, J. Limpert, H. Zellmer, A. Tünnermann, V. Reichel, K. Mörl, S. Jetschke, S. Unger, H.-R. Müller, J. Kirchhoff, T. Sandrock, and A. Harschak, “1.3 kW Yb-doped fiber laser with excellent beam quality,” in Conference on Lasers and Electro-Optics (CLEO), Postdeadline Paper CPDD2. Washington, DC, USA: Optical Society of America, 2004

[4] G. P. Agrawal, Nonlinear Fiber Optics, 3rd ed. San Diego, CA, USA: Academic Press, 2001.

[5] J. Limpert, N. Deguil-Robin, I. Manek-Hönninger, F. Salin, F. Röser, A. Liem, T. Schreiber, S. Nolte, H. Zellmer, A. Tünnermann, J. Broeng, and A. Petersson, “High-power rod-type photonic crystal fiber laser,” Optics Express, vol. 13, no. 4, pp. 1055–1058, 2005.

[6] [6] V. V. Ravi Kanth Kumar, A. K. George, W. H. Reeves, J. C. Knight, and J. Russell, “Extruded soft glass photonic crystal fiber for ultrabroad supercontinuum generation,” Optics Express, vol. 10, no. 25, pp. 1520–1525, 2002.

[7] Y. Chen, Y. Ren, X. Qu, D. Yang, and Y. Wang, “Highly efficient Yb-doped double clad photonic crystal fiber by melting technology,” IEEE Sensors Journal, vol. 21, no. 17, pp. 19289–19295, 2021.

[8] M. H. Rahman, M. M. Rana, M. S. Hossain, S. Sen, and M. Al Amin, “Analytical approach for modeling and simulation of photonic crystal

fiber based on low effective material loss," SN Applied Sciences, vol. 5, p. 71, 2023.

[9] A. M. Maidi, I. Yakasai, P. E. Abas, M. M. Nauman, R. A. Apong, S. Kaijage, and F. Begum, "Design and simulation of photonic crystal fiber for liquid sensing," 2021.

[10] G. Keiser, Optical Fiber Communications, 4th ed. New York, NY, USA: McGraw-Hill, 2008.

[11] K. Fidanboylu and H. S. Efendioglu, "Fiber optic sensors and their applications," in Proc. 5th International Advanced Technologies Symposium (IATS'09), Karabuk, Turkey, 2009.

[12] L. Bansal, Development of a fiber optic chemical sensor for detection of toxic vapors, Ph.D. dissertation, Drexel Univ., Philadelphia, PA, USA, 2004.

[13] R. Buczyński, "Photonic crystal fibers," Acta Physica Polonica A, vol. 106, no. 2, 2004.Thévenaz, L. (2011). Advanced fiber optics: Concepts and technology. EPFL Press.

[14] B. Zsigri, Photonic crystal fibers as the transmission medium for future optical communication systems, Ph.D. dissertation, Technical Univ. of Denmark, Kongens Lyngby, Denmark, 2006.

[15] T. Ritari, Novel sensor and telecommunication applications of photonic crystal fibers, Ph.D. dissertation, Helsinki Univ. of Technology, Helsinki, Finland, 2006.

[16] H. Valtna-Lukner, J. Repän, S. Valdma, and P. Piksarv, "Endlessly single-mode photonic crystal fiber as a high-resolution probe," Applied Optics, vol. 55, no. 33, pp. 9407–9411, 2016.

[17] N. M. Mortensen, J. Folkenberg, and A. Bjarklev, "Mode field radius of photonic crystal fiber expressed by V-parameter," Optics Letters, vol. 28, no. 23, pp. 2309–2311, 2003.

[18] S. Olyaee and F. Taghipour, "A new design photonic crystal fiber with ultraflattened dispersion to simultaneously minimize the dispersion and confinement loss," Journal of Physics: Conference Series, vol. 276, Proceedings of the 3rd International Photonics and Optoelectronics Meeting (POE), 2011.

[19] G. Renversez and B. Kuhlmey, "Dispersion management with microstructured optical fibers: Ultraflattened chromatic dispersion with low losses," Optics Letters, vol. 28, no. 12, pp. 989–991, 2003.

[20] K. P. Hansen, J. R. Jensen, C. Jacobsen, H. R. Simonsen, J. Broeng, P. M. W. Skovgaard, A. Petersson,

and A. Bjarklev, “Highly nonlinear photonic crystal fiber with zero-dispersion at 1.55 µm,” Optics Express, Optical Society of America, 2002.

[21] K. Ahmed, M. J. Haque, M. A. Jabin, B. K. Paul, I. S. Amiri, and P. Yupapin, “Tetra-core surface plasmon resonance based biosensor for alcohol sensing,” Physica B: Condensed Matter, vol. 570, pp. 48–52, 2019

[22] M. M. Bilal, S. Lopez-Aguayo, and A. Thottoli, “Numerical analysis of solid-core photonic crystal fiber based on plasmonic materials for analyte refractive index sensing,” Photonics, vol. 10, no. 10, p. 1070, 2023.

[23] W. Jin, H. F. Xuan, and H. L. Ho, “Sensing with hollow-core photonic bandgap fibers,” Measurement Science and Technology, vol. 21, no. 9, p. 094014, 2010.

[24] N. Chen, M. Zhao, Y. Zhu, L. Gao, C. Lu, X. Sun, X. Ding, and X. Wang, “Design and simulation of a simple-structure and high-performance plasmonic polarization filter based on gold layers deposited on photonic crystal fiber,” Micromachines, vol. 16, no. 10, p. 1088, 2025, doi: 10.3390/mi16101088.